Multiple-order reflections from monochromating crystals for the collection of X-ray absorption spectra at extremely high energies

F. D'Acapito,[a]* S. Colonna,[b] C. Maurizio[c] and S. Mobilio[d,e]

[a]INFM, Operative Group in Grenoble, c/o European Synchrotron Radiation Facility, GILDA CRG, BP 220, F-38043 Grenoble, France, [b]CNR, Istituto di Struttura della Materia, c/o European Synchrotron Radiation Facility, GILDA CRG, BP 220, F-38043 Grenoble, France, [c]INFM, Dipartimento di Fisica, Universita di Padova, Via Marzolo 8, I-35131 Padova, Italy, [d]Istituto Nazionale di Fisica Nucleare – LNF, PO Box 13, I-00044 Frascati, Italy, and [e]Universita 'Roma Tre', Dipartimento di Fisica, Via della Vasca Navale 84, I-00146 Roma, Italy. E-mail: dacapito@esrf.fr

A simple method to collect X-ray absorption spectra at extremely high energies (≥ 50 keV) is presented. The method is based on the use of the third harmonic signal from a conventional double-crystal monochromator. Strengths and limitations of the method are shown, together with a few experimental examples on metallic foils and oxide powders in transmission and fluorescence mode.

Keywords: extended X-ray absorption fine structure (EXAFS); *K* edges; rare earths; 5*d* metals.

1. Introduction

X-ray absorption spectroscopy (XAS) is a particularly powerful technique for the determination of the local structure around a given chemical species. The technique is used in a wide range of disciplines from solid-state physics to chemistry from biology to earth sciences (Lee *et al.*, 1981). The method is based on the interference between the wave associated with a photoelectron ejected by an atom (photoabsorber) after the absorption of an X-ray photon of energy E and the waves scattered backwards by the surrounding atoms.

Given that the initial state is well localized on the photoabsorber site and that the core hole is sufficiently long lived, the interference effect appears in the X-ray absorption spectra as oscillations superimposed on the atomic background and can be used for quantitative structural determinations.

The advent of third-generation synchrotrons has marked a great advance in the energy region accessible for XAS owing to the high energy of the electron beam that determines high critical energies of the sources (bending magnets, wigglers). However, new problems in data collection and data treatment are encountered that are not present at lower energies. Namely, the lifetime of the hole in the ionized level strongly decreases with Z (Krause & Oliver, 1979) giving rise to a broadening effect that can be of the order of $\Gamma = 40$ eV FWHM for the inner states (1*s*) of heavy elements (rare earths, 5*d* metals). This effect tends to cancel the fine structures in the absorption coefficient even in the extended region. For this reason it was initially surprising when fine structures were observed above the *K* edge of high-Z elements like Ce (Asakura *et al.*, 1986). However, as previously pointed out (Borowski *et al.*, 1999), the broadening effect is constant in E space whereas the XAS oscillations are periodic in the photoelectron wavevector space, $k \propto (E - E_0)^{1/2}$, where E_0 is the edge value. This implies that only the initial part of the spectrum is severely affected by the lifetime broadening and that XAS spectra can be collected provided that a wide k range is measured. Owing to this limitation, XAS at high energies cannot be used as a substitute of more conventional *L*-edge XAS but can be useful in a variety of cases when the co-presence of atomic species with interfering edges prevents the collection of a good spectrum. On a synchrotron beamline it is crucial to have easy access to photon energies above 40 keV for the collection of such spectra without losing access to lower energies where most of the work is performed. In this paper we present a simple method to solve this problem based on the use of third-harmonic reflection of the monochromator crystals.

2. Experimental method

The selection of high energy from the white spectrum of a typical bending magnet (BM) or wiggler source is made by using Si perfect crystals. The use of high-order diffracting planes [like Si(511)] is reported for this kind of applications both for flat (Asakura *et al.*, 1986; Nishihata *et al.*, 1998, 2001; Borowski *et al.*, 1999) or sagittally focusing (Braglia *et al.*, 1998; Colonna *et al.*, 2000) geometries. Owing to the flux enhancement (Pascarelli *et al.*, 1996), the latter method is more indicated for studies on diluted samples or thin films. However, there are some experimental difficulties to be considered when planning to run a beamline at high energy. First of all, even when working with high-order crystal planes, the incidence angles become very low, which causes problems in monochromator positioning accuracy and energy resolution. The energy resolution ΔE at energy E (with a corresponding angle θ_B) induced by an angular spread $\Delta\theta$ is given by

$$\Delta E = \frac{E}{\tan\theta_B}\Delta\theta. \quad (1)$$

Equation (1) can also be applied to derive the energy step ΔE relative to an angular step $\Delta\Theta$. For example, at 80 keV for an Si(511) crystal the Bragg angle is $\sim 4.2^\circ$ and a typical goniometer single step (usually 10^{-4} deg) corresponds to 2 eV. A 1 mm total-width slit placed at 37 m [typical values for the GILDA CRG beamline at the European Synchrotron Radiation Facility (ESRF)] results in a resolution of 29 eV.† An alternative way is to exploit the high-order reflection of lower-order planes: for example, the Si(933) reflection can be used with Si(311)-cut crystals. In this way it is possible to work at relatively low angles with less influence of the beam divergence and angular resolution. Considering again the 80 keV case, the Bragg angle is 8.1°, the minimum step is 1 eV and the resolution is 15 eV. Another important aspect to consider is that in this way no intervention on the beamline (crystal change) is needed to switch from a low-energy to a high-energy configuration. The main problem with this method is the presence of several energies in the beam such as the fundamental, the fourth and higher-order harmonics that can heavily affect the quality of the spectrum. However, their influence can be limited by using proper filters and selecting a suitable part of the total beam pattern. Indeed, a 350 µm Cu filter attenuates the fundamental by a factor of 100 at 80 keV whereas, owing to a different extinction length in the Si crystals (80 µm at 26 keV and 660 µm at 80 keV), the third harmonic is shifted upwards with respect to the fundamental. For the fourth (and higher) harmonic, the lower emission intensity from the machine (a factor of three for the ESRF

† Energy resolutions have to be regarded as full width at half-maximum values as we consider the full width of the slit. In a Gaussian picture it corresponds to 2.35σ, where σ is the standard deviation.

BM) and the lower monochromator transmissivity owing to the narrower Darwin width (at 8.1°: 0.16 μrad for 80 keV and 0.09 μrad for 107 keV, the fourth harmonic) act together to limit the presence of higher orders in the spectrum. These theoretical calculations, made using the program *XOP* (Sanchez del Rio & Dejus, 1997), have been confirmed by experiment. Tests have been conducted at the GILDA beamline at ESRF in order to assess the feasibility of this technique; the monochromator was equipped with Si(311) crystals and run in sagittally focusing geometry. The energy spectrum of the scattered beam collected from an Al plate with a high-purity Ge detector showed no visible traces either of the fundamental and the fourth harmonic at 80 keV with 60% crystal detuning.

3. Examples

3.1. Transmission mode: the Au *K* edge

Here we show the possibility of collecting good quality XAS spectra at high energy by using the third-order reflection from an Si(311)-cut crystal. In this case the *K* edge of a 100 μm Au foil was collected at a temperature of 10 K. A 350 μm Cu filter was used to reject the fundamental and a couple of ion chambers filled with Kr at 1000 mbar were used to measure the absorption. The raw spectrum is shown in Fig. 1: note the rather good quality of the spectrum, the noise-to-signal ratio being only a few 10^{-4}. Figs. 2 and 3 show the EXAFS spectra and the Fourier transforms (FT) resulting from a four-shell fit. The fit of the EXAFS data was performed using the *GNXAS* code (Filipponi *et al.*, 1995; Filipponi & Di Cicco, 1995): first and second shells were included as single scattering, third and fourth shells were modelled as the sum of a single- plus a triple-scattering signal. Particular attention was devoted to the calculation of the edge jump *J*. Note that, owing to the noticeable core-hole width Γ, the initial part of the spectrum still falls in the rising part of the edge. As many extraction programs determine the jump from an extrapolation of the atomic background to the edge energy E_0, the value of *J* can easily be underestimated. A good choice is to fit the edge region (±500 eV from the edge) with a function of the type (Rohler, 1985)

$$\mu = \mathrm{Bkg} + J\left[\arctan\left(\frac{E_0 - E}{\Gamma/2}\right)\frac{1}{\pi} - \frac{1}{2}\right]$$

that gives a more proper estimate of *J*. A fit of the edge performed on the Au sample gave $J = 1.4$ [the theoretical value from the film thickness was $J = 1.3$ using the MacMaster tables (MacMaster *et al.*, 1969)] and the measured core-hole width Γ was 43 eV, in reasonable agreement with tabulated values (52 eV; Krause & Oliver, 1979). We obtained a first-shell bond length of 2.882 ± 0.003 Å, in good agreement with crystallographic data (2.8837 at RT; Wychoff, 1964). The number of first neighbours was found to be 12 ± 1 with an s_0^2 parameter of 0.85. A corresponding Debye–Waller factor of 0.0011 ± 0.0002 Å^{-2} was obtained from the fit whereas the calculated Debye–Waller factor, based on an approximation of the correlated Debye model (Sevillano *et al.*, 1979) and a value of the Au Debye temperature T_D = 160 K averaged over the results of different methods (Herbstein, 1961), is 0.0025 Å^{-2}.

3.2. Fluorescence mode: rare-earth (RE) doped glasses

The use of sagittal focusing, providing a high flux from the monochromator of about 10^8–10^9 photons s^{-1} in this energy range, is ideal for the analysis on dilute samples. In the present example the spectrum of powdered Yb_2O_3 taken at liquid nitrogen temperature (LNT) in transmission mode is compared with that taken at LNT in fluorescence mode on a silicate glass doped with Yb and Er with the

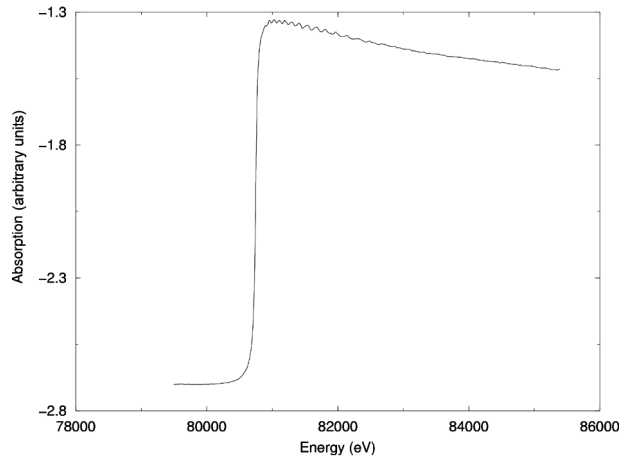

Figure 1
Absorption spectrum of a 100 μm Au foil at 10 K collected by using the Si(933) reflection.

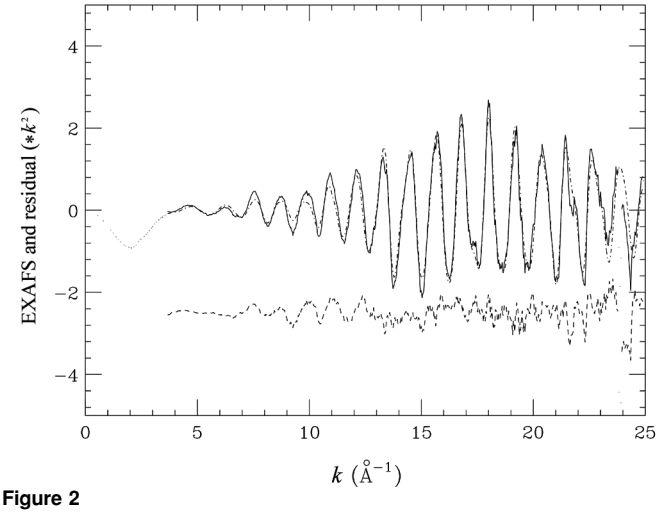

Figure 2
Fit of the EXAFS spectrum with a four-shell model (*GNXAS* code). The fit was performed in the interval 3.5–25 Å^{-1} weighting the data by k^2. Upper curves: data (continuous line) and fit (dot–dashed line). Bottom curve: residual.

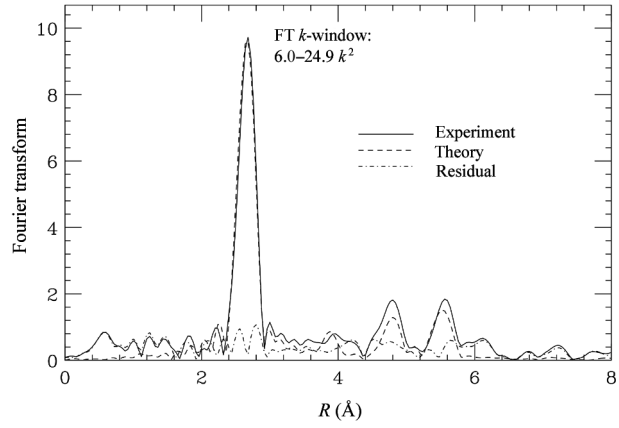

Figure 3
Fourier transform of the EXAFS data in Fig. 2.

Table 1
Quantitative results of the EXAFS analysis on Yb-doped glass and oxide.

Data for the first, second and third shell are shown in different rows.

	Yb_2O_3	Yb_2O_3 (Wychoff, 1964)	Glass
N_1	6.0 ± 0.5 O	6.0 O	6.6 ± 0.5 O
R_1 (Å)	2.26 ± 0.03	2.22	2.27 ± 0.03
N_2	6.0 ± 0.5 Yb	6.0 Yb	
R_2 (Å)	3.49 ± 0.01	3.46	
N_3	6.0 ± 0.5 Yb	6.0 Yb	
R_3 (Å)	3.99 ± 0.01	3.95	

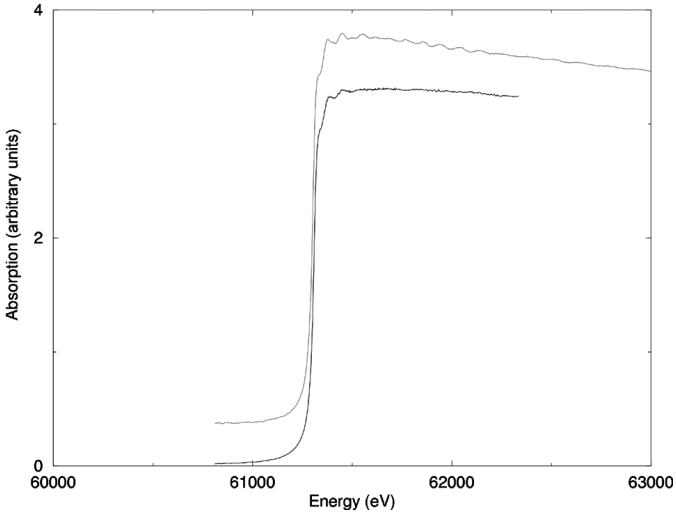

Figure 4
Absorption spectrum of a Yb_2O_3 powder (upper curve) and Yb-doped glass (lower curve) collected by using the Si(933) reflection. The two curves have been rescaled and shifted vertically for clarity. Note the oscillations in the region around 62 keV present in the crystal spectrum and absent in the glass spectrum.

aim of detecting evidence of possible Yb–RE pair correlations. Glasses were prepared by the sol–gel method (Almeida, 1998) and had a composition of 72 mol% SiO_2, 18 mol% TiO_2, 8.25 mol% Al_2O_3, 0.875 mol% Er_2O_3 and 0.875 mol% Yb_2O_3. Powdered glass was deposited on a millipore membrane resulting in the equivalent of a 100 µm-thick sample; RE density was estimated to be 10^{18} RE cm^{-2}. An extensive discussion for the scientific case of this experiment as well as the XAS data at the Er *K* edge can be found elsewhere (D'Acapito *et al.*, 2001). The fluorescence signal was detected by a multi-element high-purity germanium detector with digital signal processing. In this case, the use of the *K* edges was mandatory to obtain a wide *k*-range spectrum to check in a stringent way for the presence of Yb–RE correlations, which are readily visible above $k = 10$ Å^{-1}. Indeed, only a limited range ($k_{max} \simeq 9$ Å^{-1}) is obtainable from the Yb L_{III} edge owing to the presence of the Er L_{II}. The EXAFS spectra and the relative FT are shown in Figs. 4 and 5. A quantitative analysis of the transmission and fluorescence spectra has been performed, this time with the *FEFF8* package (Ankudinov *et al.*, 1998). The results are resumed in Table 1 with the crystallographic data taken from Wychoff (1964). A general agreement can be noted between the two data sets of Yb_2O_3 leading to the conclusion that commonly used data-analysis programs work correctly also in this energy range. Moreover, this investigation has permitted us to rule out the presence of Yb–RE pair correlations in the doped silicate

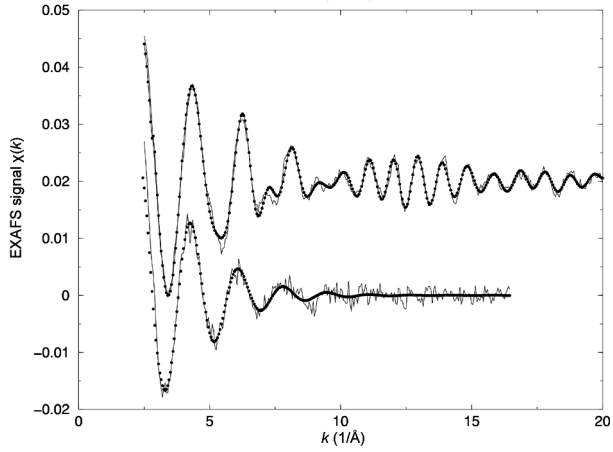

Figure 5
Fit (dots) of the EXAFS spectra (line) with a three-shell model for the crystalline Yb_2O_3 and with a one-shell model for the glass sample. Oscillations above $k = 10$ Å^{-1} visible in the crystalline sample arise from RE–RE coordination and are absent in the glass. Data collected using the Si(933) reflection.

glass owing to the absence of oscillations above 10 Å^{-1}. Such oscillations are present in the Yb_2O_3 XAS spectrum.

4. Conclusion

In this paper we have demonstrated that the third-harmonic signal from Si(311) crystals can be used for the collection of reliable XAS spectra at very high energies. This method, although needing care to eliminate undesired signals from the fundamental and fourth harmonic, is very useful, permitting experimentalists to cover a very wide energy range with a single Si(311) crystal pair. Quantitative results, in agreement with crystallographic determinations, can be extracted from data taken both in transmission and fluorescence mode.

The GILDA CRG beamline is jointly financed by CNR, INFM and INFN. The authors thank Professor R. Almeida and Dr L. Santos of the INESC Institute in Lisboa for providing the Er/Yb-doped glasses.

References

Almeida, R. M. (1998). *J. Sol-Gel Sci. Technol.* **13**, 51–59.
Ankudinov, A. L., Ravel, B., Rehr, J. J. & Conradson, S. D. (1998). *Phys. Rev. B*, **58**, 7565–7576.
Asakura, K., Satow, Y. & Kuroda, H. (1986). *J. Phys (Paris) Colloq.* **47**(C8), 185–188.
Borowsky, M., Bowron, D. T. & De Panfilis, S. (1999). *J. Synchrotron Rad.* **6**, 179–181.
Braglia, M., Dai, G., Mosso, S., Pascarelli, S., Boscherini, F. & Lamberti, C. (1998). *Appl. Phys. Lett.* **83**, 5065–5068.
Colonna, S., Arciprete, F., Balzarotti, A., Balestrino, G., Medaglia, P. G. & Petrocelli, G. (2000). *Physica C*, **334**, 64–76.
D'Acapito, F., Mobilio, S., Santos, L. & Almeida, R. (2001). *Appl. Phys. Lett.* **78**, 2676–2678.
Filipponi, A., Di Cicco, A. & Natoli, C. R. (1995). *Phys. Rev. B*, **52**, 15122–15134.
Filipponi, A. & Di Cicco, A. (1995). *Phys. Rev. B*, **52**, 15135–15149.
Herbstein, F. H. (1961). *Adv. Phys.* **10**, 313–355.
Krause, M. O. & Oliver, J. H. (1979). *J. Phys. Chem. Ref. Data*, **8**, 329–338.
Lee, P. A., Citrin, H. & Eisenberger, P. (1981). *Rev. Mod. Phys.* **6**, 769–806.
MacMaster, W. H., Kerr del Grande, N., Mallett, J. H. & Hubbell, J. H. (1969). *Compilation of X-ray Cross Sections*, Report UCRL-50174, §II, Revision 1.

Lawrence Livermore National Laboratory, University of California, Livermore, CA 94550, USA.
Nishihata, Y., Kamishima, O., Kubozono, Y., Maeda, H. & Emura, S. (1998). *J. Synchrotron Rad.* **5**, 1007–1009.
Nishihata, Y., Mizuki, J., Emura, S. & Uruga, T. (2001). *J. Synchrotron Rad.* **8**, 294–296.
Pascarelli, S., Boscherini, F., D'Acapito, F., Hrdy, J., Meneghini, C. & Mobilio, S. (1996). *J. Synchrotron Rad.* **3**, 147–155.
Rohler, J. (1985). *J. Magn. Mag. Mater.* **47**/**48**, 175–180.
Sanchez del Rio, M. & Dejus, R. J. (1997). *Proc. SPIE*, **3152**, 148–157.
Sevillano, E., Meuth, H. & Rehr, J. J. (1979). *Phys. Rev. B*, **20**, 4908–4911.
Wychoff, R. N. G. (1964). *Crystal Structures.* New York: Wiley.

Received 14 May 2001 • Accepted 6 December 2001